Liquid Crystals
Publication details, including instructions for authors and subscription information:
http://www.informaworld.com/smpp/title~content=t713926090

Invited Lecture. Matrix liquid-crystal display device technologies

S. Matsumoto[a]; H. Hatoh[a]; A. Murayama[a]
[a] Electron Device Engineering Laboratory, Toshiba Corporation, Yokohama, Japan

To cite this Article Matsumoto, S. , Hatoh, H. and Murayama, A.(1989) 'Invited Lecture. Matrix liquid-crystal display device technologies', Liquid Crystals, 5: 5, 1345 — 1364
To link to this Article: DOI: 10.1080/02678298908027772
URL: http://dx.doi.org/10.1080/02678298908027772

LIQUID CRYSTALS, 1989, VOL. 5, NO. 5, 1345–1364

Invited Lecture

Matrix liquid-crystal display device technologies

by S. MATSUMOTO, H. HATOH and A. MURAYAMA
Electron Device Engineering Laboratory, Toshiba Corporation, 8 Shinsugita-cho, Isogoku, Yokohama, 235 Japan

Our recent studies of ferroelectric chiral smectic and super-twisted nematic (ST) multiplexed-matrix liquid-crystal displays (LCDs) and a thin-film-transistor (TFT) active-matrix twisted nematic (TN) LCD are presented, mainly in terms of liquid-crystal material and cell optimization. This is based on a consideration of their electro-optical characteristics. In addition the matrix LCD devices developed through these studies are introduced, including a 12-inch-diagonal video-rate multicolour ferroelectric LCD, a highly multiplexed genuine achromatic ST LCD with a single cell and a 4-inch-diagonal full-colour a-Si TFT-addressed TN LCD for a video display.

1. Introduction

A considerable amount of work is currently directed towards the realization of a liquid-crystal display (LCD) that has both a large information content and a high display quality comparable to a cathode-ray-tube display. Ferroelectric chiral smectic and super-twisted nematic (ST) multiplexed-matrix LCDs and a thin-film-transistor (TFT) active-matrix twisted nematic (TN) LCD may be the most promising candidates for such a realization.

Here we present our recent studies on these multiplexed-matrix and active-matrix LCDs, mainly in terms of a liquid-crystal material and cell optimization based on their electro-optical characteristics consideration. We also introduce the matrix LCD devices developed through these studies, including a 12-inch-diagonal video-rate multicolour ferroelectric LCD, a highly multiplexed genuine achromatic ST LCD with a single cell and a 4-inch-diagonal full-colour a-Si TFT-addressed TN LCD for a video display.

2. Video-rate multicolour ferroelectric LCD

Ferroelectric liquid-crystal (FLC) displays using a chiral smectic C (S_C^*) material have received great interest, because they have a high multiplexing capability, based on their bistability and fast response time, and they have considerable potential for realization of a large-area flat-panel colour TV. We have already developed for the first time a 12-inch-diagonal multicolour FLC display [1]. However, its operating frame frequency was less than a video rate and, in addition, the contrast ratio was not sufficient.

In this section we describe an improved multicolour FLC display with 639 × 400 pixels with a 12-inch-diagonal size, which operates at a video rate of a 33·3 Hz frame frequency under a 1/400 duty cycle multiplexing and has a high contrast ratio. This improvement is based on the following achievements:

0267–8292/89 $3.00

(1) a new S_C^* FLC mixture FLC-025: this shows a fast response time, definite bistability and uniform alignment;

(2) a plural-line erasing drive method: this gives a high-frame-frequency capability and a large operating voltage margin;

(3) an LCD panel construction with ITO electrodes patterned on R.G.B. colour filters in a black matrix: this construction is effective in preventing distortion of the applied-voltage waveforms and in increasing the contrast ratio.

2.1. *Ferroelectric liquid-crystals*

Many properties of FLC need to be optimized in order to realize a highly multiplexed large-area FLC display; these are as follows.

(1) For wide-temperature operation, an FLC is required to have a broad S_C^* temperature range, for example from $-20°C$ to $+60°C$.

(2) To achieve uniform alignment over a large area with a conventional rubbing method, an FLC should exhibit isotropic (I)–chiral-nematic (N*)–smectic A (S_A)–S_C^* phase-transition sequence as well as the long N* and S_C^* helical pitches [1].

(3) A fast response time is essential for multiplexing at a high frame frequency. In order to improve the response time, it is effective to increase the spontaneous polarization P_s as well as to decrease the rotational viscosity.

(4) The bistability is a prerequisite for a multiplexing drive. An FLC with too large a P_s cannot exhibit bistability. Thus there exists a limit to improving the response time by increasing the P_s value. We have estimated the limiting value of P_s to be about $20\,nC/cm^2$.

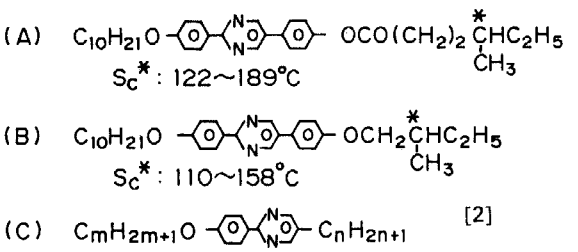

[2]

Figure 1. Representative components of an FLC mixture FLC-025.

In order to fulfil these requirements, we have prepared an FLC mixture, FLC-025. It consists of a new class of 2,5-diphenylpyrimidine FLCs, non-chiral S_C liquid crystals and chiral dopants; these components are shown in figure 1. They play the following roles in the FLC mixture:

(i) 2,5-diphenylpyrimidine FLCs broaden the S_C^* temperature range and compensate the helical pitches;
(ii) non-chiral S_C liquid crystals decrease the rotational viscosity, as well as P_s;
(iii) chiral dopants increase the P_s value.

The physical properties of FLC-025 are summarized in table 1. A $2\,\mu m$ thick test cell with a rubbed polyimide alignment layer was used in the electro-optical measurements.

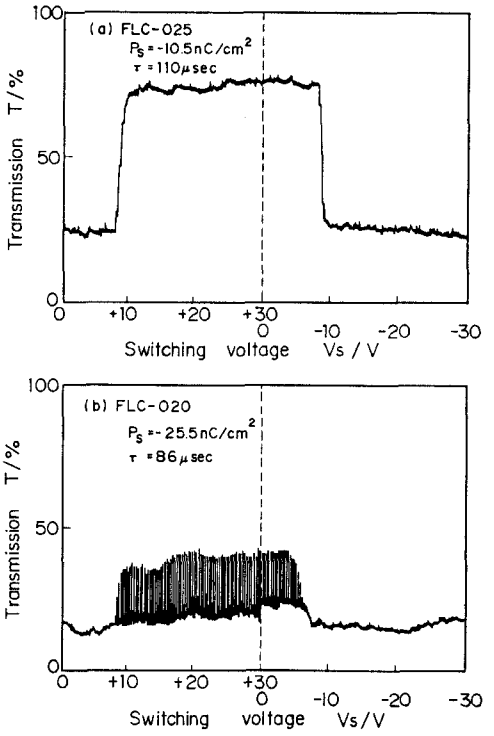

Figure 2. Bistability threshold curves for the FLC mixtures FLC-025 and FLC-020, using pulse width $t = 100\,\mu s$.

Table 1. Physical properties of an FLC mixture of FLC-025.

Transition temperature °C	77 N* 71 S_A 62 S_C^*–20 C
Spontaneous polarization, P_s nC cm^{-2}	10·5 (polarity minus)
Tilt angle, θ/°	24·0
S_C^* helical pitch/μm	6 (at 25°C)
N* helical pitch/μm	60 (at 73°C)
Response time τ/μs	110 ($\pm$ 10 V square wave)
Bistability threshold voltage V_{th}/V	8·7 (100 μs pulse width)

Figure 2 shows the bistability threshold curves of the FLC mixtures FLC-025 with a moderate P_s and FLC-020 with a large P_s. FLC-025 shows definite and symmetric bistability behaviour, while FLC-020 shows very poor bistability. These threshold curves were obtained by applying the bipolar reset and switching pulses shown in figure 3, where the reset-pulse amplitude is fixed at $\pm$ 30 V and the switching pulse is swept from 0 V to $\pm$ 30 V.

Figure 4 shows the relation between the bistability threshold voltage V_{th} and the switching pulse width t for FLC-025 at 25°C. This relation is particularly important for determining the multiplexing-drive condition, since the bistability threshold voltage is associated with the driving voltage and the switching pulse width is related to the operating frame-frequency.

As we have described, the FLC mixture FLC-025 with a moderate P_s value has a wide S_C^* temperature range, a favourable phase-transition sequence as well as long N* and S_C^* helical pitches, fast response time and good bistability threshold behaviour.

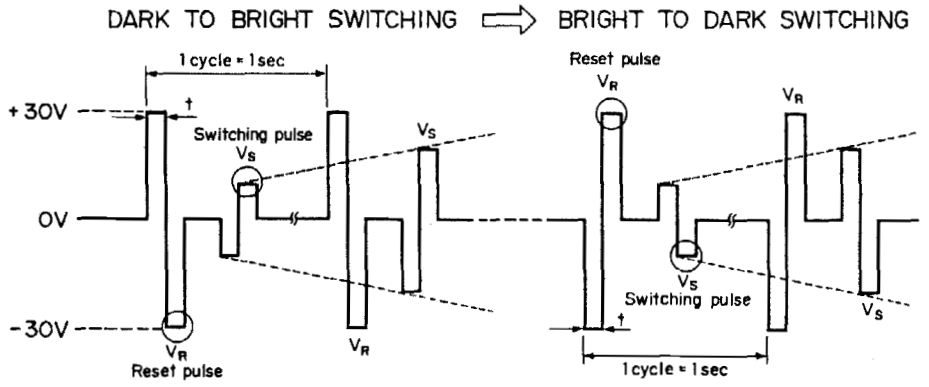

Figure 3. Pulse waveforms for the evaluation of bistability threshold behaviour.

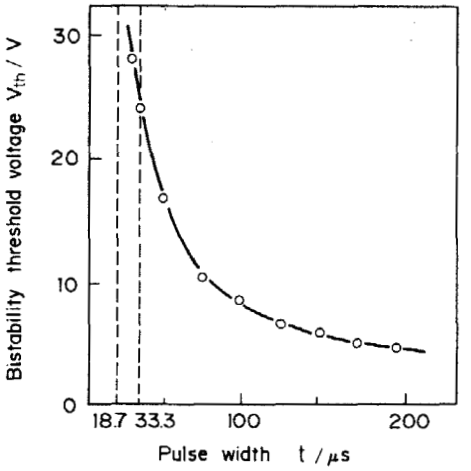

Figure 4. Relation between the bistability threshold voltage V_{th} and the switching pulse width t for FLC-025.

2.2. *Multiplexing-drive method*

Figure 5(*a*) shows a conventional multiplexing-drive method which is called the two-field writing method [3]. Its frame frequency is given by

$$f = 1/(2tN \times 2), \tag{1}$$

where N is the number of scanning lines and t is the pulse width. So, for 400 lines (a 1/400 duty cycle), the frame frequency is

$$f_1 = 1/1600t. \tag{2}$$

The multicolour ferroelectric LCD developed is driven with a different drive method, shown in figure 5(*b*); we call this the plural-line erasing drive method [4]. For this method, n scanning lines are written simultaneously to a dark (erased) state before each line is written line by line to a bright state. Its frame frequency f is therefore given by

$$f = \left[2tN\left(1 + \frac{1}{n}\right)\right]^{-1}. \tag{3}$$

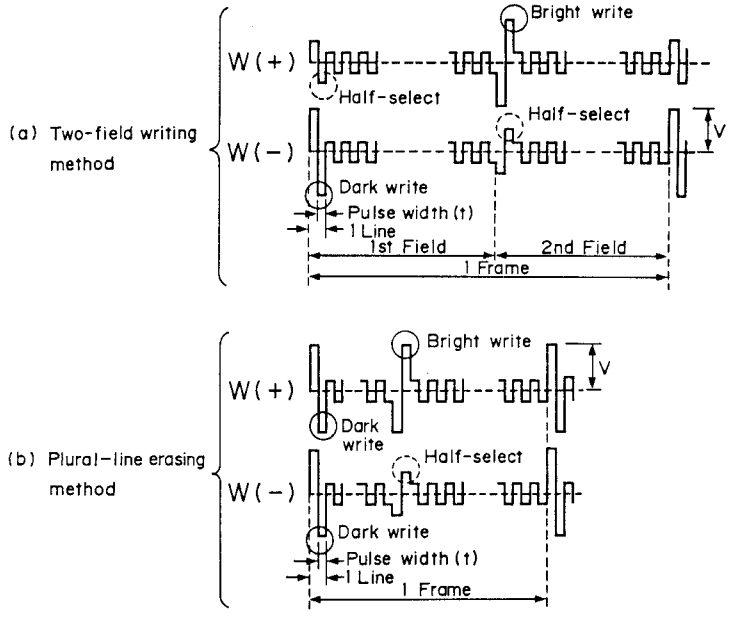

Figure 5. Two kinds of drive waveforms for multiplexing an FLC cell.

The LCD developed has 400 scanning lines and is driven by an eight-line erasing method. The frame frequency is therefore given by

$$\begin{aligned} f_2 &= [800t(1 + \tfrac{1}{8})]^{-1} \\ &= 1/900t. \end{aligned} \tag{4}$$

From equations (2) and (4), we can see that the frame frequency with the plural-(eight-) line erasing method can become $f_2/f_1 = 16/9$ times as high as that with the two-field writing method. Accordingly, in order to achieve a video-rate operation ($f = 33{\cdot}3$ Hz) at a duty cycle of 1/400, the required pulse width t is $33{\cdot}3\,\mu$s for the plural-line erasing method, while it is $18{\cdot}7\,\mu$s for the two-field writing method. It is therefore evident from figure 4 that the combination of the plural-line erasing method and the fast-response FLC mixture FLC-025 can achieve a video-rate operation, while the two-field writing method cannot operate the FLC mixture at a video-rate frame frequency, since the driving voltage is limited, practically, at around 30 V with conventional ICs for LCDs. Thus the plural-line erasing method is suitable for a large information content video-rate FLC display because of the high-frame-frequency operating capability as well as the large operating-voltage margin. The question of the operating-voltage margin will be described elsewhere.

2.3. *LCD panel construction*

Figure 6 shows schematically the panel construction for the multicolour FLC display developed. The cell thickness is $2\,\mu$m. The alignment layer is polyimide and its rubbing directions are parallel. ITO electrodes were patterned on RGB colour filters in order to prevent the distortion of applied-voltage waveforms across a FLC layer and an adverse voltage drop due to capacitive coupling. In addition, the colour filters are equipped with a black matrix to increase the contrast ratio.

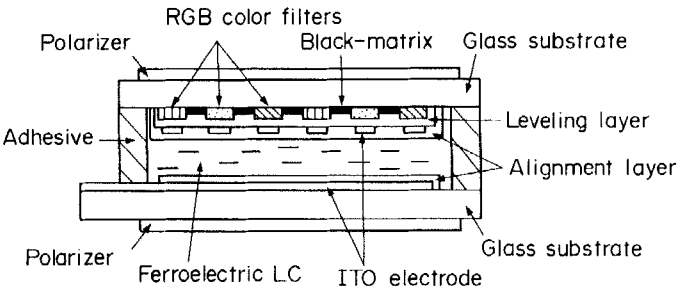

Figure 6. Panel construction of the multicolour FLC display developed.

2.4. *Video-rate multicolour ferroelectric LCD*

On the basis of this work, we have developed a 12-inch-diagonal, video-rate multicolour ferroelectric LCD; table 2 summarizes its specifications. The FLC mixture FLC-025 fills the panel. It has 639 × 400 pixels with RGB colour filters in a black matrix, and the active display area is 243 × 182 mm^2. The panel is driven by the plural-line erasing method (see figure 5(*b*)) at a multiplexing duty cycle of 1/400. The driving voltage is 30 V and the bias ratio is 1/4. The frame frequency is 33·3 Hz at room temperature (25°C), which corresponds to a driving pulse width t = 33·3 μs.

Figure 7 shows photographs of the multicolour (eight colours) images displayed by this ferroelectric LCD, which operates at a video-rate frame frequency of 33·3 Hz at room temperature.

Table 2. Specifications of the multicolour FLC display.

Panel size/mm^2	260 × 200
Active display area/mm^2	243 × 182
Matrix configuration/pixels	639 × 400
Pixel pitch/mm	0·38, 0·46
Colour filters	RGB mosaic in a black matrix
Duty ratio	1/400
Driving voltage/V	30
Frame frequency/Hz	33·3
Pulse width/μs	33·3
Maximum contrast ratio	7 : 1

3. Single-cell genuine achromatic ST LCD

A super-twisted nematic liquid-crystal display (ST LCD) whose twist angle is larger than about 180° has attracted a great deal of attention as a practically favourable LCD with both a large contrast ratio and a wide viewing angle. Nevertheless, a standard ST LCD cannot realize an achromatic, i.e. black and white, display appearance. The basic principle of an ST LCD results in interference colours in the off state; the so-called yellow-mode ST LCD displays black figures on a yellow background and the blue-mode ST LCD has white figures on a blue background [5]. These interference colours are not accepted by everybody and they are also undesirable for a multicolour-display application based on the combination of an ST LCD and colour filters. In consequence, intensive attempts to realize an achromatic ST LCD have continued, including the investigation of ST LCDs based on low optical retardation [6–9], a double-cell [10] and guest–host modes [11]. Of these, a double-cell ST (D-ST) LCD has the best black and white display appearance as well as the highest contrast ratio.

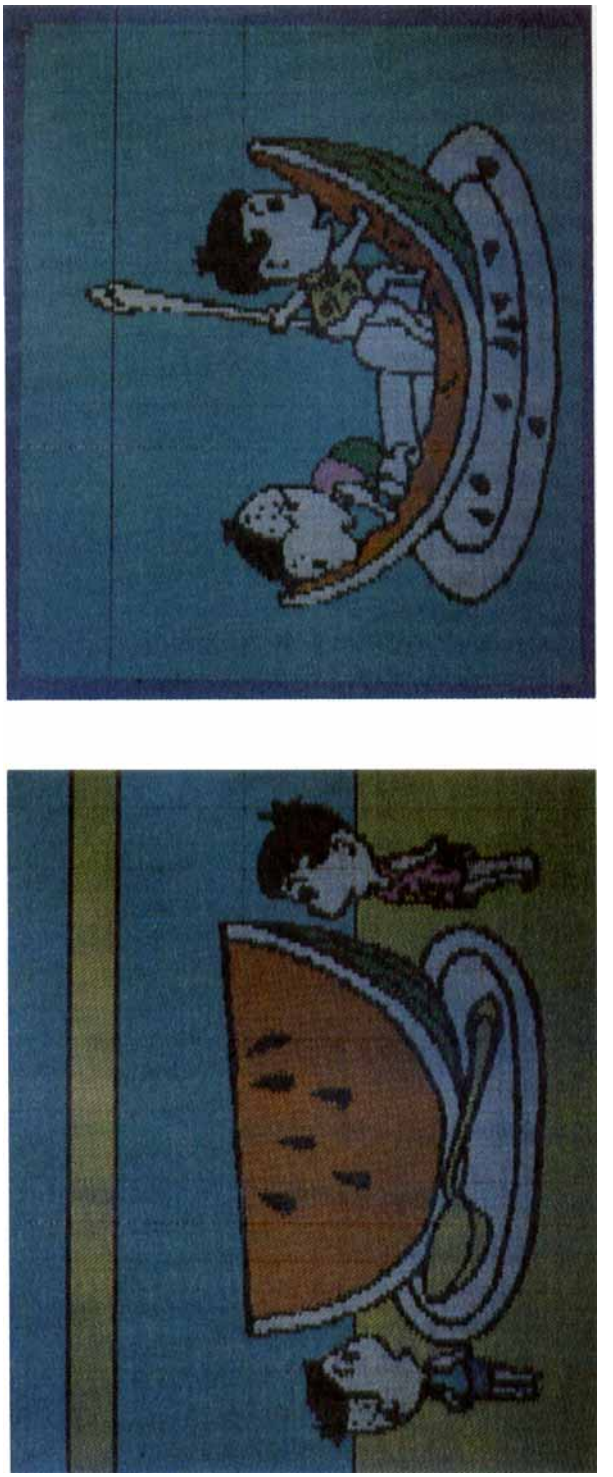

Figure 7. Photographs of multicolour images obtained with the ferroelectric LCD with 639 × 400 pixels and 12-inch-diagonal in size.

However, in a D-ST LCD, an additional LC cell with the opposite twist sense, having the same retardation as the operating ST cell, is needed to compensate the optical path difference in the operating cell. Accordingly, a D-ST LCD has serious problems; it is thick, heavy and expensive, i.e. has a low production yield, because of its double-cell construction.

Recently, we have successfully developed a genuine achromatic ST LCD characterized by single-cell construction. It employs an optical retardation film (RF) of a stretched polymer, instead of an additional LC cell as for a D-ST LCD. The developed retardation film ST (RF-ST) LCD realizes not only an excellent black and white display appearance, a high contrast ratio and a good viewing angle, comparable to those of a D–ST LCD, but also such favourable features as light weight, thin design and low cost because of its single-cell construction. Here we present the electro-optical characteristics and display performance of this RF–ST LCD.

3.1. *Calculation of the optical characteristics in an RF–ST LCD*

Figure 8 shows the basic construction of an RF–ST LCD. An optical retardation film (RF) is set between the ST LC cell and polarizer. The wavelength dependence of transmission in an RF–ST LCD was calculated by Berremann's 4 × 4 matrix method, varying the cell condition including the retardation of the RF R, the angle of the RF axis A, the angles of the front and rear polarizer axes P_f, P_r and $\Delta n\,d$ of the LC cell. Figure 9 shows the definition of the angles A, P_f and P_r. The twist angle of the LC cell was fixed at 240°.

Figure 10(*a*) shows the calculated wavelength dependence of the off-state ($V = 0$) transmission T_{off} in an RF–ST LCD with $\Delta n\,d = 0{\cdot}67\,\mu$m, $P_f = 115°$, $P_r = 93°$ and $A = 85°$, as a function of the retardation value of the RF from $R = 350$ nm to $R = 500$ nm. Figure 10(*b*) presents the corresponding dependence of the on-state transmission T_{on}, i.e. the select state transmission in a multiplexing drive. $R = 450$ nm, these figures show that the off-state transmission is sufficiently low and almost independent of wavelength and also that the on-state transmission is relatively high and substantially flat. These calculated results with a 450 nm RF are consistent with the experimentally measured wavelength dependence of the off and on states in an RF-ST LCD; this is shown by open circles in figures 10(*a*) and (*b*). From these studies, it is readily seen that a high-quality black and white display appearance can be achieved with an RF with $R = 450$ nm.

In the same way, we have investigated the electro-optical characteristics in an RF–ST LCD with plural retardation films. These studies show that such an RF–ST

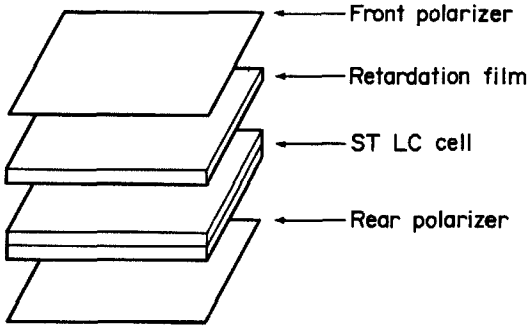

Figure 8. Schematic view of an RF-ST LCD construction.

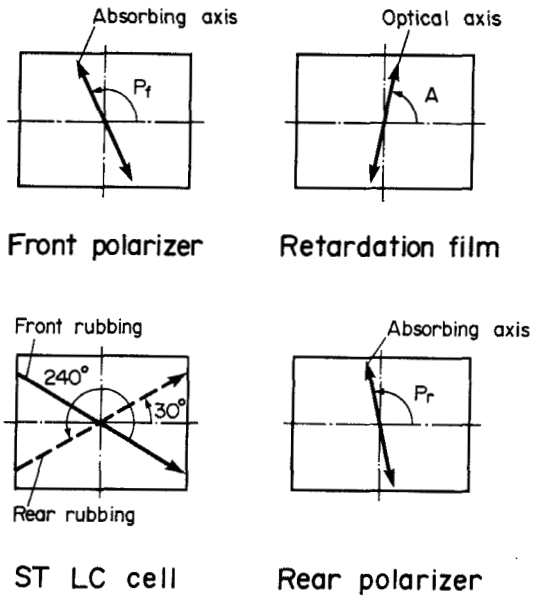

Figure 9. Angle definition of the optical axes in an RF–ST LCD.

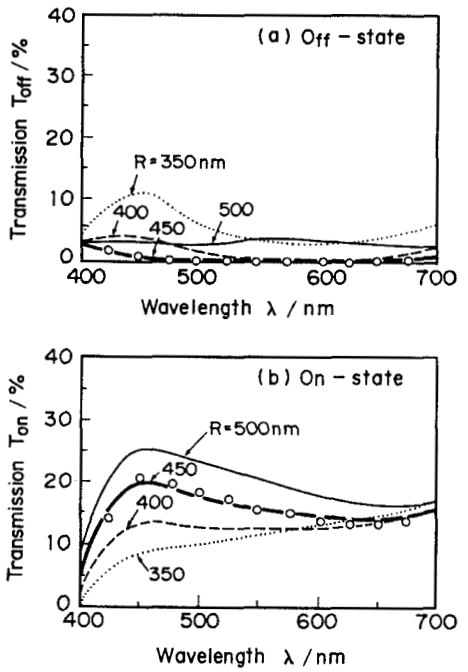

Figure 10. Calculated and measured on- and off-state transmission spectra in an RF–ST LCD with a different retardation RF.

LCD has a more achromatic display appearance and a higher contrast ratio than an RF–ST LCD with a single RF. On the basis of this finding, a high-quality black and white RF–ST LCD has been successfully developed, by using plural retardation films; we call this a monochrome–ST (M–ST) LCD, hereinafter.

Table 3. Specifications of the M–ST LCD.

Panel size/mm^2	235(H) × 157(V)
Active display area/mm^2	211(H) × 132(V)
Matrix configuration/pixels	640(H) × 400(V)
Pixel pitch/mm	0·33(H), 0·33(V)
Display mode	Transmissive mode
Back light	Fluorescent lamp
Operating duty cycle	1/200
Contrast ratio	20 : 1
Viewing angle/°	50 cone (CR > 5)
Response time/ms	190

3.2. *Display performance of an M–ST LCD*

The specifications of the M–ST LCD developed are summarised in table 3. Its display-panel size is 11-inch diagonal and it has 640 (horizontal) × 400 (vertical) pixels. It is driven by a 1/200 duty multiplexing way.

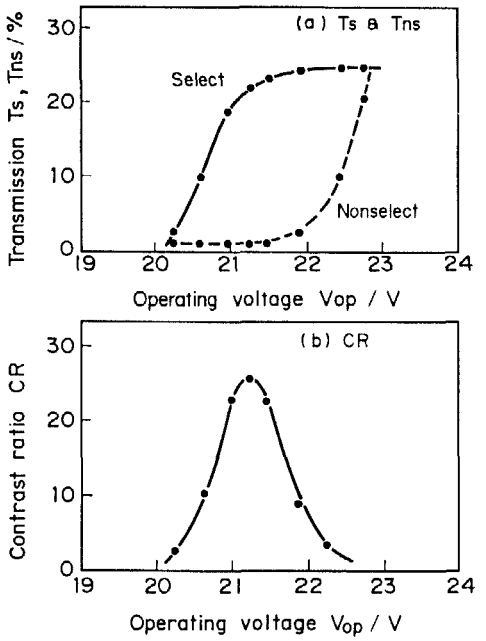

Figure 11. Transmission T_s and T_{ns} of the select and non-select states (*a*) and contrast ratio CR (*b*) versus operating voltage in the M–ST LCD.

Figure 11(*a*) shows the operating-voltage dependence of transmission T_s and T_{ns} at normal incidence in the select (solid curve) and non-select (dashed curve) states with a 1/200 duty multiplexing drive. Figure 11(*b*) shows the operating voltage dependence of the contrast ratio CR. The maximum contrast ratio is 25 : 1 and the corresponding transmission in the select state is more than 20 per cent. Thus the M–ST LCD developed achieves a large contrast ratio as well as a bright display appearance.

Figure 12 gives the transmission T_s and T_{ns} spectra in the select (solid curve) and non-select (dashed curve) states under a 1/200 duty multiplexing drive. The transmission in the non-select state is almost independent of wavelength and sufficiently low. The transmission in the select state is sufficiently large and substantially flat,

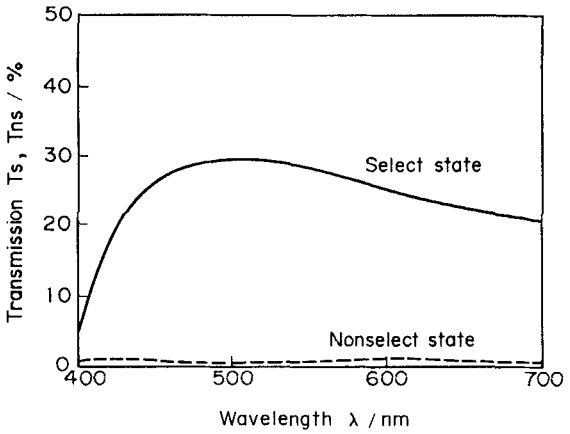

Figure 12. Transmission spectra of the select and non-select states in the M-ST LCD.

being independent of wavelength. These results mean that the M-ST LCD developed has a genuine black and white display appearance and is also very useful for producing a high-quality colour LCD combined with RGB colour filters.

Figure 13 shows the black and white images displayed by the M-ST LCD developed, which operates with a duty cycle of 1/200.

4. a-Si TFT-addressed TN LCD for a video display

Various active-matrix-addressed LCDs have emerged as extremely useful and promising candidates to overcome the multiplexing limitation of conventional multiplexed-matrix LCDs and also to realize both a high information content and a good display quality, comparable to a CRT display. Such active-matrix LCDs use either three-terminal switching devices, such as a-Si [12], poly-Si [13] and CdSe [14] thin-film transistors (TFTs), or two terminal switching devices like double diodes [15, 16] and metal-insulator-metal [17]. Some types of active-matrix LCDs are already under production, and small-sized TV sets employing such LCDs, mainly an a-Si TFT-addressed LCD based on a twisted nematic (TN) mode, are now commercially available.

In this section we describe our studies on the optimization of cell conditions in a TFT-addressed TN LCD from the viewpoint of its video-display application. The essential studies include the influence of alignment layers on the voltage-retention capability, the deviation of the practical first-minimum condition from the theoretical one and the influence of the pretilt angle and the polarizer arrangement on the electro-optical characteristics and display performance. An a-Si TFT-addressed TN LCD for a colour video display developed on the basis of these studies will be also presented; this has 220 × 480 pixels and a four-inch-diagonal size.

4.1. *Alignment influence on voltage-retention capability*

It is a prerequisite for a TFT-addressed liquid-crystal display (LCD) that the voltage across the cell supplied through a TFT is held during a frame time. A poor voltage-retention capability causes a low contrast ratio and often a flicker problem as well. In this section the influence of the alignment layer on the voltage-retention capability in a TN LCD is described.

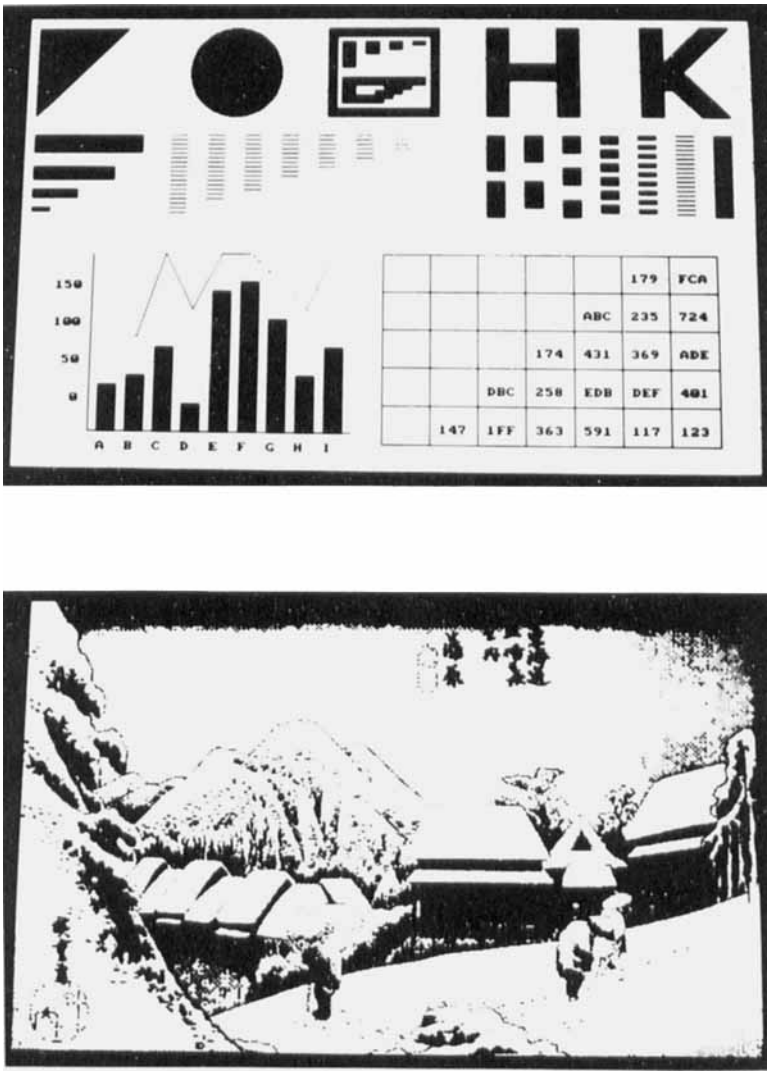

Figure 13. Photograph of black and white images displayed by the M-ST LCD with 640 × 400 pixels in an 11-inch-diagonal size.

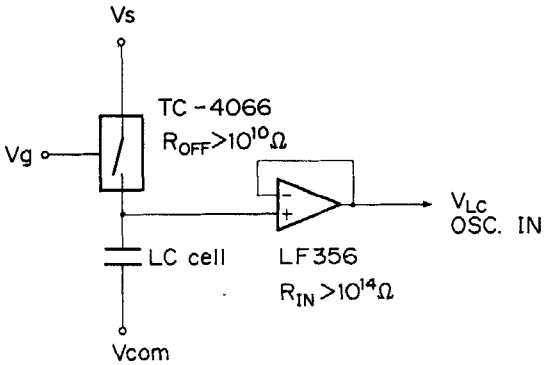

Figure 14. circuit diagram for measurement of the voltage-retention capability in a LC cell.

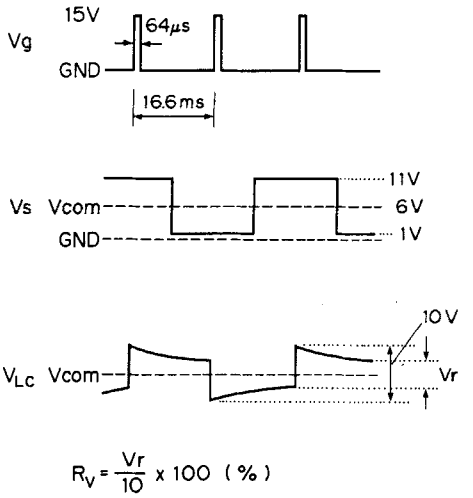

Figure 15. Waveforms of the gate voltage V_g and signal voltage V_s, together with the voltage change V_{LC} across an LC layer.

Figure 14 shows the measurement circuit used to investigate the voltage-retention capability in a simple LC cell without TFTs. An analogue transistor switch (TC-4066) is used, instead of a TFT, and its output terminal is connected to an electrode of the LC cell, which corresponds to a pixel electrode in a TFT-addressed LCD. When the gate voltage V_g is applied to the analogue switch, the signal voltage V_s is transferred to the pixel electrode. The common voltage V_{com} is always applied to the other electrode of the cell, which corresponds to a common electrode in a TFT LCD. The potential difference between the pixel and the common electrodes is applied to a LC layer, and its change with time is monitored by a storage oscilloscope through a buffer circuit with an operational amplifier (LF 356).

The waveforms of V_g and V_s, together with the change of the voltage across a LC layer V_{LC}, are shown in figure 15. The gate pulse width of 64 μs and its interval of 16·6 ms correspond respectively to the addressing time for each line and the frame time in a TFT LCD for a video display. The signal voltage V_s is ± 5 V to the level of $V_{com} = 6$ V. The voltage-retention capability R_v is defined by

$$R_v = \frac{V_r}{10} \times 100 \text{ per cent}, \tag{5}$$

where V_r is the voltage retained after the frame time. Figure 16 shows the voltage-retention capabilty R_v in a simple TN LC cell with various alignment layers. The LC material used belongs to a high-resistivity PCH class and has a resistivity higher than $10^{12}\,\Omega$cm. Cell A with an obliquely evaporated SiO alignment layer gives a large R_v, while cells B and C with a rubbed layer of different polyimide PI(1) and PI(2) have a definitely small R_v. However, it should be noted that cell D with a non-rubbed PI(1) layer has a large R_v, comparable to that of the SiO evaporated cell A. The large R_v with cell A may be due to a clean process of evaporation, that is, an alignment process characterized by both non-contact with the substrate surface and purification treatment of SiO. This clean alignment process may have no adverse influence on the resistivity of a LC layer. On the other hand, the small R_v with the rubbed PI cells B and C may be due to some contamination on the substrate surface caused by the

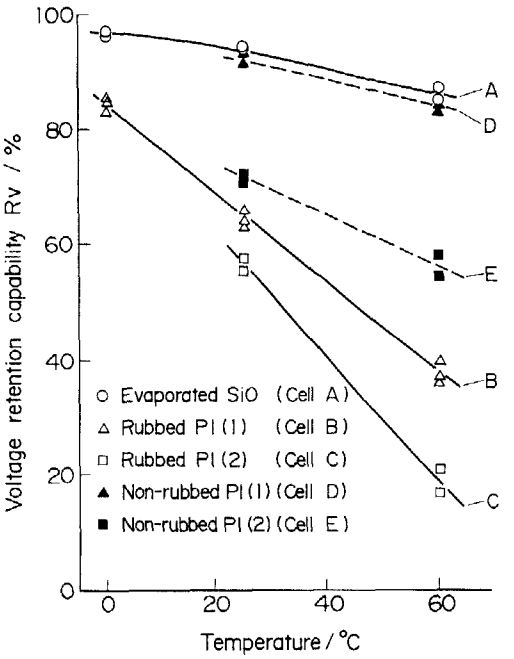

Figure 16. Voltage-retention capability in a TN cell with five kinds of alignment layers.

rubbing treatment of a contact process. This contamination may reduce the resistivity of the LC layer.

Thus the large R_v observed in the cell D with a PI(1) layer may be explained by the absence of a rubbing treatment. Nevertheless, cell E with a non-rubbed PI(2) layer has a relatively small R_v. This may be due to the reduction of a LC-layer resistivity caused by PI(2) itself. According to a calculation assuming that the voltage across an LC layer varies exponentially with time, the LC resistivities of $10^{12}\,\Omega$ cm and $10^{10}\,\Omega$ cm correspond to voltage-retention capabilities R_v of 96 and 68 per cent respectively.

These results demonstrate that it is essential to a TFT-addressed LCD not only to use a high-resistivity LC material but also to employ a high-purity alignment material and a suitable alignment method.

4.2. *Optimum condition of retardation* $\Delta n\,d$

The off-state transmission T_{off} in a TN LC cell with a normal black polarizer arrangement is given by the Gooch–Tarry equation [18]. In a TFT-addressed TN LCD the first-minimum $\Delta n\,d$ condition ($2\Delta n\,d/\lambda = \sqrt{3}$) is preferred in order to improve the viewing angle and response time as well as to achieve a large contrast ratio, while the second-minimum condition ($2\Delta n\,d\lambda = \sqrt{15}$) is generally used in a conventional multiplexed-matrix TN LCD in order to achieve a steep electro-optic response [19].

Accordingly, it seems in general, very important to adjust the retardation $\Delta n\,d$ value precisely to the theoretical first-minimum condition to achieve the largest contrast ratio and the best colour reproducibility. Nevertheless, we have found, as shown in figure 17, that the transmission T_{off} in an actual TN LC cell is a minimum at a definitely larger $\Delta n\,d$ condition than the theoretical first-minimum condition.

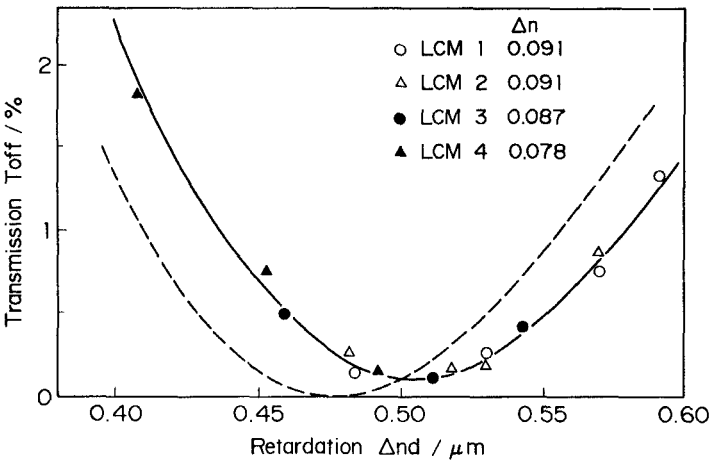

Figure 17. Experimental (solid curve) and calculated (dashed curve) relations between the off-state transmission T_{off} and retardation $\Delta n\,d$ in a TN LC cell.

Figure 17 shows the experimentally observed relation between T_{off} and $\Delta n\,d$ in various TN LC cells (solid curve), together with the calculated relation (dashed curve). The cell thickness ranged from 5·0 μm to 6·5 μm, and four different classes of LC materials (LCM 1–4) with various birefringences Δn were used. A small pretilt angle of 2° was applied and so its influence on $\Delta n\,d$ is negligible. The polarizers were set in a normal black arrangement and a 550 nm pass filter was used. From figure 17, it is readily recognized that the experimental transmission T_{off} becomes a minimum at $\Delta n\,d$ = 0·505 μm, and this value is definitely large compared with the theoretical value $\Delta n\,d$ = 0·476 μm. This deviation between the experimental and theoretical results may be explained by the existence of some disordered liquid-crystal layer near the substrate surface, which cannot contribute to the optical rotatory power in a TN cell [20]. The disordered-layer thickness is estimated to be about 0·15 μm from each substrate surface, since the difference in $\Delta n\,d$ is 0·03 μm and the birefringence of the LC materials is about 0·1.

These results show that, in order to achieve the largest contrast ratio and the best colour reproducibility in a TFT-addressed TN LCD, it is important to optimize the $\Delta n\,d$ condition by taking account of the deviation of the practical first-minimum condition from the theoretical one.

4.3. *Influence of pretilt angle on electro-optical characteristics*

Good controllability of grey levels, together with fast response time and wide viewing angle, are essential for a video display. In this section studies of the influence of the pretilt angle on the electro-optical characteristics in a TN LCD, such as the grey scale, viewing angle, operating voltage and response time, are described.

TN cells with three kinds of alignment layers were prepared. The first low-pretilt cell had a rubbed polyimide layer and its pretilt angle was 2°. The second, medium, one had an obliquely evaporated SiO layer and its pretilt angle was 16°. The third also had the SiO layer, but it had a higher pretilt angle of 25°. The cells were filled with the same LC material with Δn = 0·091 (LCM 1) and their cell thickness was nominally 5·5 μm. Polarizers were set in a normal white arrangement.

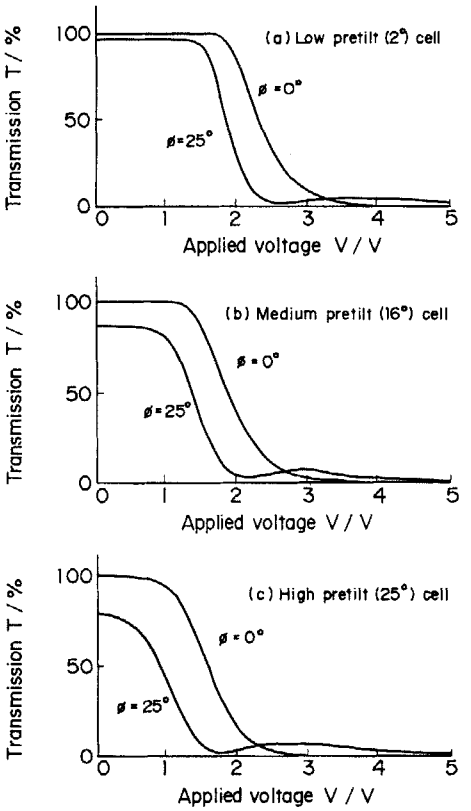

Figure 18. Electro-optical response curves in a TN LC cell with various pretilt angles at viewing angles 0° and 25°.

Table 4. Electro-optical characteristics in a TN cell with different pretilt angles.

LC cell	Pretilt angle/°	Threshold voltage V_{th}/V	Steepness γ/%	Viewing angle dependence β/%	Response times τ_{on}/ms	Response times τ_{off}/ms
Low-pretilt cell	2	1·85	58	27	40	17
Medium-pretilt cell	16	1·40	88	37	30	20
High-pretilt cell	25	1·05	107	49	30	30

The transmission in these cells with different pretilt angles of 2°, 16° and 25° were measured at viewing angles of 0° and 25° to the substrate normal, with an applied voltage from 0 V to 5 V. The results are shown in figures 18(*a*), (*b*) and (*c*), and table 4 summarizes the threshold voltage V_{th}, steepness γ and viewing angle dependence β for each cell, obtained from these figures. V_{th}, γ and β are defined by

$$V_{th} = V(T = 90 \text{ per cent}, \phi = 0°), \tag{6}$$

$$\gamma = \frac{V(10 \text{ per cent}, 0°) - V(90 \text{ per cent}, 0°)}{V(90 \text{ per cent}, 0°)}, \tag{7}$$

$$\beta = \frac{2[V(50 \text{ per cent}, 0°) - V(50 \text{ per cent}, 25°)]}{V(50 \text{ per cent}, 0°) + V(50 \text{ per cent}, 25°)}, \tag{8}$$

where $V(T, \phi°)$ denotes the voltage at which the transmission reaches T (per cent) at viewing angle $\phi(°)$. The transmission with no applied voltage at $\phi = 0°$ is defined as $T = 100$ per cent.

With increasing pretilt angle, V_{th} decreases and γ increases. These result in a low-voltage operation and easily controlled grey levels. However, β increases with increasing pretilt angle and, as a result, the viewing angle becomes narrow. As shown in table 4, the response time τ_{on} decreases with increasing pretilt angle, while the response time τ_{off} increases. τ_{on} and τ_{off} are defined as the times for the normal incident transmission to change by 90 per cent at an applied voltage $V(T = 10$ per cent, $\phi = 0°)$.

These results show that it is essential to a TN LCD for video display to optimize the pretilt angle by considering its influence on the electro-optical characteristics such as the threshold voltage V_{th}, the steepness γ, the viewing-angle dependence β and the response times τ_{on} and τ_{off}.

4.4. *Influence of polarizer arrangement on display performance*

The display performance of a TN LCD is greatly influenced by the polarizer arrangement, namely, a normal white (crossed polarizers) or a normal black (parallel polarizers) arrangement. In this section some work on the influence of the polarizer arrangement on the contrast ratio and the viewing angle in a TN LCD is described.

Figures 19(*a*) and (*b*) show the viewing-angle dependence of the contrast ratio (CR) in vertical and horizontal directions in a TN LCD with different applied voltages, for normal white polarizer arrangement. On the other hand, figures 20(*a*) and (*b*) show the corresponding viewing-angle dependence of CR in case of a normal black polarizer arrangement. The LC cell used has a rubbed polyimide alignment layer and is filled with a LC material with $\Delta n = 0{\cdot}091$ (LCM 1). The cell thickness is $5{\cdot}5\,\mu$m, so as to employ the first-minimum condition. CR is defined as the ratio of the transmission in the on state to that in the off state. For a normal white arrangement, the contrast ratio curve is greatly influenced by the viewing angle as well as by the applied voltage, although the maximum contrast ratio is very large. On the other

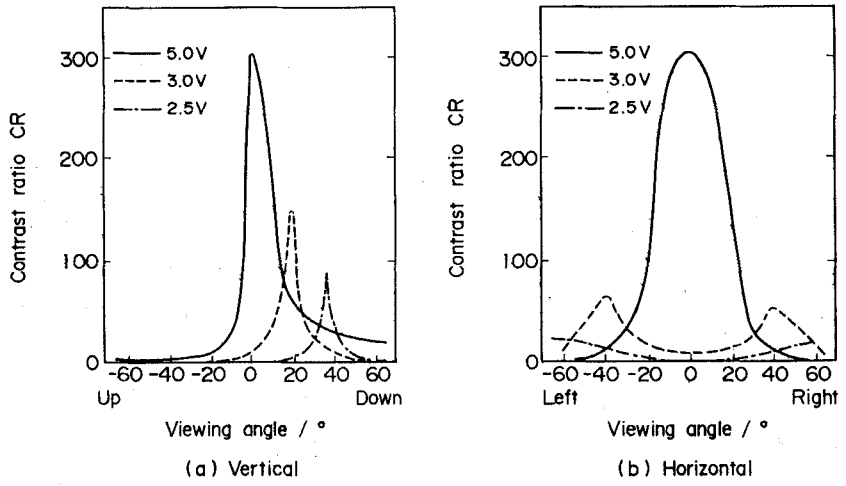

Figure 19. Viewing-angle dependence of the contrast ratio (CR) in a TN LCD with a normal white polarizer arrangement.

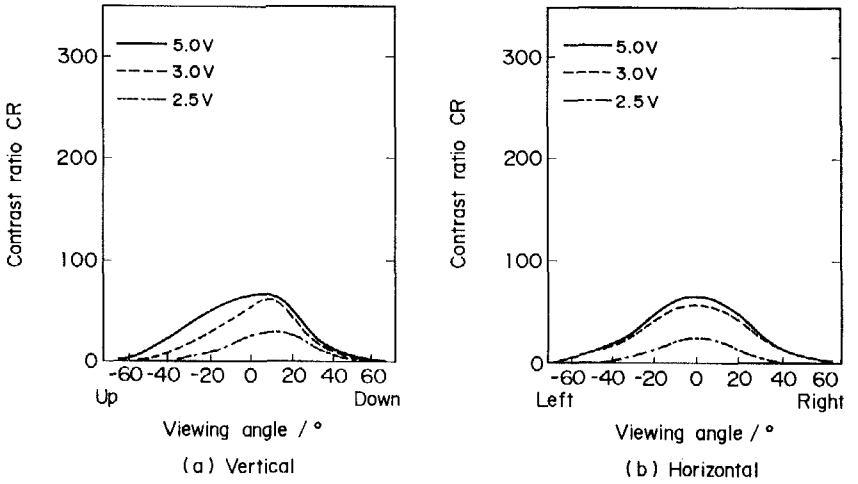

Figure 20. Viewing-angle dependence of the contrast ratio (CR) in a TN LCD with a normal black polarizer arrangement.

hand, in a normal black case, the maximum contrast ratio is definitely small, but the viewing-angle dependence of CR is not large.

In addition to these facts, there is another significant difference between the display performances of normal white and black polarizer arrangements, as we now describe. In general, the off-state transmission spectrum in a TN LCD changes with a $\Delta n\, d$ deviation from the first-minimum condition, as suggested by the Gooch–Tarry equation. In a normal black case, this spectrum change exerts a significantly adverse effect on the dark level of the transmission and results in poor colour reproducibility, in addition to a definite decrease of the contrast ratio. On the other hand, in a normal white case, such a change in the transmision spectrum is not a serious problem, because the change has an effect on the bright level, but not on the dark level.

From this, it is readily recognized that the polarizer arrangement in a TFT-addressed TN LCD for a video display must be selected by considering the difference of display performance, such as the contrast ratio, its viewing-angle dependence and the colour reproducibility, between normal white and black arrangements.

4.5. *a-Si TFT-addressed TN LCD for colour video display*

On the basis of the studies described here, we have developed an a-Si TFT-addressed LCD for a colour video display. Its specifications and display performance

Table 5. Specifications and performance of the a-Si TFT-addressed LCD for use in a colour TV display.

Display mode	Transmissive TN (normal white)
Driving method	a-Si TFT-matrix addressing
Display area/mm^2	60·5 (V) × 80·6 (H) (4 in. diagonal)
Number of pixels	220 (V) × 480 (H)
Pixel pitch/μm^2	257 (V) × 168 (H)
Colour filters	RGB triangular in a black matrix
Contrast ratio	More than 100 : 1
Response times/ms	$\tau_{on} + \tau_{off} = 55$
Viewing angle/°	55 (V); 80 (H) (CR > 10 : 1)

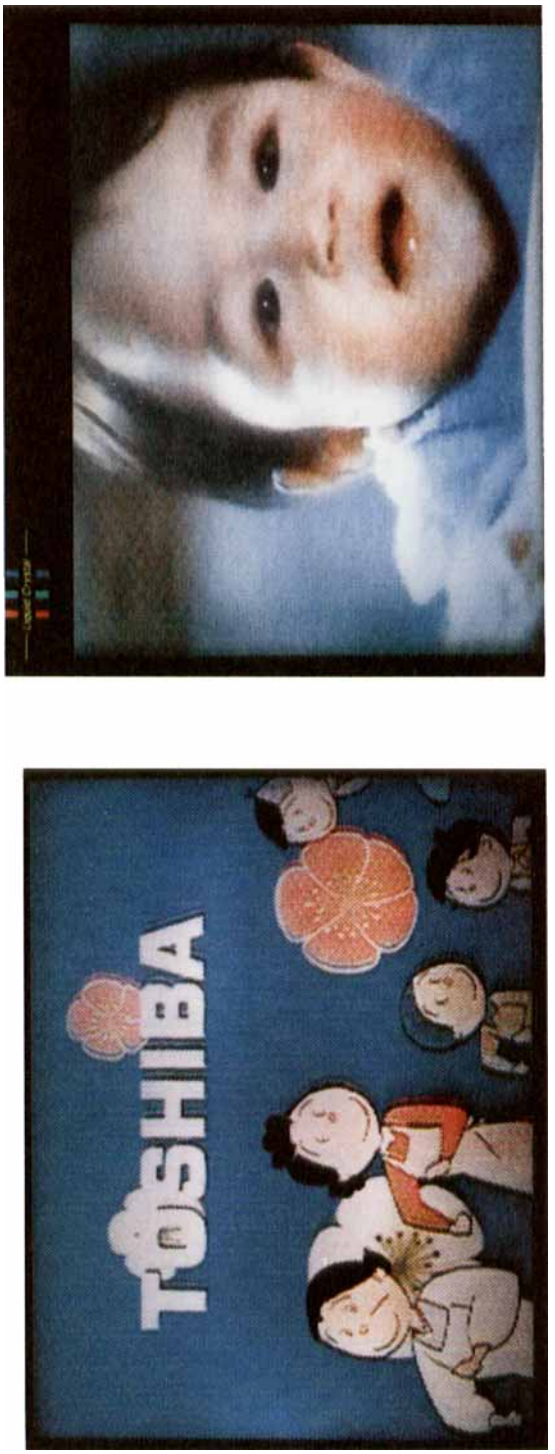

Figure 21. On-the-air TV colour images obtained with the 4-inch-diagonal a-Si TFT-addressed LCD with 240 × 480 pixels.

are summarized in table 5. It is based on a transmissive and normal white TN mode. This colour video LCD has 220 × 480 pixels with RGB colour filters in a black matrix. The active display area is a four-inch-diagonal. The maximum contrast ratio is more than 100 : 1 and the total response time ($\tau_{on} + \tau_{off}$) is 55 ms. The vertical and horizontal viewing angles are 55° and 80° respectively, where the contrast ratio is more than 10 : 1. Figure 21 demonstrates some on-the-air TV colour images obtained with the TFT-addressed LCD.

References

[1] MATSUMOTO, S., HATOH, H., KAMAGAMI, S., and MURAYAMA, A., 1987, Invited Lecture L5 at the 1st International Symposium on Ferroelectric Liquid Crystals, Bordeax; *Ferroelectrics*, in press. HATOH, H., MURAYAMA, A., KAMAGAMI, S., and MATSUMOTO, S., 1987, *Proc. SID*, **28**, 205.

[2] ZASCHKE, H., 1975, *J. prac. Chem.*, **317**, 617.

[3] HARADA, T., TAGUCHI, M., IWASA, K., and KAI, M., 1985, *SID'85 Digest of Technical Papers*, p. 131.

[4] SHIMIZU, K., TANAKA, Y., SEKIKAWA, K., INOUE, K., and HORI, H., 1987, *Proc. SID*, **28**, 211.

[5] SCHEFFER, T. J., NEHRING, J., KAUFMANN, M., and AMSTUTZ, H., 1985, *SID'85 Digest of Technical Papers*, p. 400.

[6] SCHADT, M., and LEENHOUTS, F., 1987, *Appl. Phys. Lett.*, **50**, 236.

[7] KAWASAKI, K., YAMADA, K., WATANABE, R., and MIZUNOYA, K., 1987, *SID'87 Digest of Technical Papers*, p. 391.

[8] HATOH, H., SHOJI, M., YAMAMOTO, T., and MATSUMOTO, S., 1987, *Tech. Rep. ITE Japan*, **11**, 43.

[9] HATOH, H., SHOJI, M., and MATSUMOTO, S., 1988, *Molec. Crystals liq. Crystals*, **163**, 101.

[10] KATOH, K., ENDO, Y., AKATSUKA, M., OHGAWARA, M., and SAWADA, K., 1987, *Jap. J. appl. Phys.*, **26**, L1784.

[11] *Nikkei Micro Device*, **10**, 79 (1987).

[12] YANAGISAWA, T., KASAHARA, K., OKADA, Y., SAKAI, K., KOMATSUBARA, Y., FUKUI, I., MUKAI, N., IDE, K., MATSUMOTO, S., and HORI, H., 1984, *Proceedings of the 4th International Display Research Conference (Eurodisplay '84)*, p. 265.

[13] OANA, Y., 1984, *SID'84 Digest of Technical Papers*, p. 312.

[14] LUO, F. C., PATTERSON, J., BRAUNSTEIN, T., and LEKSELL, D., 1985, *SID'85 Digest of Technical Papers*, p. 286.

[15] TOGASHI, S., SEKIGUCHI, K., TANABE, H., YAMAMOTO, E., SORIMACHI, K., TAJIMA, E., WATANABE, H., and SHIMIZU, H., 1984, *SID'84 Digest of Technical Papers*, p. 324.

[16] SZYDLO, N., CHARTIER, E., PERBET, J. N., PROUST, N., MAGARINO, J., and HARENG, M., 1983, *Proceedings of the 3rd International Display Research Conference (Japan Display '83)*, p. 416.

[17] MOROZUMI, S., OHTA, T., ARAKI, R., SONEHARA, T., KUBOTA, K., ONO, Y., NAKAZAWA, T., and OHARA, H., 1983, *Proceedings of the 3rd International Display Research Conference (Japan Display '83)*, p. 404.

[18] GOOCH, C. H., and TARRY, H. A., 1975, *J. Phys.* D, **8**, 1575.

[19] MATSUMOTO, S., HATOH, H., and TOMII, H., 1988, *Molec. Crystals liq. Crystals*, **163**, 87.

[20] WU, S., and EFRON, U., 1986, *Appl. Phys. Lett.*, **48**, 624.